Molecular Pharmacology Fast Forward. Published on July 27, 2005 as doi: 10.1124/mol.105.013359
This article has not been copyedited and formatted. The final version may differ from this version.

MOL (13359)

Charged residues of the conserved DRY triplet of the vasopressin V1a receptor provide molecular determinants for cell surface delivery and internalization

Stuart R. Hawtin

Institute of Cell Signalling, School of Biomedical Sciences, Queen's Medical Centre, University of Nottingham, NG7 2UH, UK.

Molecular Pharmacology Fast Forward. Published on July 27, 2005 as DOI: 10.1124/mol.105.013359
This article has not been copyedited and formatted. The final version may differ from this version.

Running title page

Running title: Mutational analysis of vasopressin V1a receptor DRY motif

Address correspondence to: Dr. Stuart Hawtin, Institute of Cell Signalling, University of Nottingham, Queen's Medical Centre, Nottingham, NG7 2UH, UK. Tel: 44-(0)115 9709282; Fax: 44-(0)115 9704493; e-mail: Stuart.Hawtin@nottingham.ac.uk

Number of text pages: 41

Number of tables: 2

Number of figures: 7

Number of references: 40

Number of words in Abstract: 250

Number of words in Introduction: 736

Number of words in Discussion: 1497

ABBREVIATIONS: AR, adrenergic receptor; AVP, [arginine^{8}]vasopressin; CA, cyclic antagonist d$(CH_2)_5$Tyr(Me)^{2}AVP; DMEM, Dulbecco's modified Eagles medium; FCS, fetal calf serum; GnRH, gonadotropic releasing hormone; GPCR, G-protein-coupled receptor; HA, hemagglutinin; HEK, human embryonic kidney; H_2R, histamine H_2 receptor; IC2, second intracellular loop; InsP, inositol phosphate; $InsP_3$, inositol 1,4,5 trisphosphate; LA, linear antagonist phenylacetyl-*D*-Tyr(Me)^{2}Arg^{6}Tyr$(NH_2)^{9}$AVP; mAChR, muscarinic receptor; NDI, nephrogenic diabetes insipidus; OT, oxytocin; OTR, oxytocin receptor; TM, transmembrane helix; SR49059, (2S)-[(2R-3S)-(5-chloro-3-(2-chlorophenyl)-1-(3,4-dimethoxybenzene-sulfonyl)-3-hydroxy-2,3-dihydro-1H-indole-2-carbonyl]-pyrrolidine-2-carboxamide; V_{1a}R, vasopressin V_{1a} receptor; V_{1b}, vasopressin V_{1b} receptor; V_2R, vasopressin V_2 receptor.

Molecular Pharmacology Fast Forward. Published on July 27, 2005 as DOI: 10.1124/mol.105.013359
This article has not been copyedited and formatted. The final version may differ from this version.

Abstract

The highly conserved "Asp-Arg-Tyr" triplet in the distal region of the third transmembrane region of most G-protein-coupled receptors is implicated in their activation process and mediation of G-protein signaling. The aim of this study was to determine if specific features at this locus are important for the vasopressin V_{1a} receptor ($V_{1a}R$) by performing site-directed mutagenesis. In transfected HEK 293T cells, mutation of Asp (D148A) resulted in a misfolded receptor that was non-functional, localized intracellularly and was not constitutively active. Non-conservative (D148R) substitution was not expressed, whereas asparagine (D148N) partially restored cell surface expression, although no specific ligand-binding or inositol phosphate signaling was detected. In contrast, conservative (D148E) substitution was expressed moderately higher, bound ligands and signaled similarly to a hemagglutinin epitope-tagged wild-type receptor. However, D148E showed a greater tendency to be internalized once it was delivered to the membrane. Individual replacements of the conserved arginine and tyrosine (R149A, Y150A) led to decreased signal transduction without affecting surface expression, agonist affinity, internalization or increasing basal signaling activity. Incorporation of aspartate (R149D) or reversal of charges (R148D/R149D) were non-functional, localized intracellularly and indicated the absence of an ionic interaction between Asp-148 and Arg-149. Interestingly, an important role of arginine was identified for regulating agonist-mediated internalization when a histidine (R149H) was present. This mutant was expressed on the cell surface but was rapidly internalized following agonist treatment. This study highlights the importance of specific charged residues within this motif which provide important determinants for cell surface delivery, internalization and for normal $V_{1a}R$ function.

Molecular Pharmacology Fast Forward. Published on July 27, 2005 as DOI: 10.1124/mol.105.013359
This article has not been copyedited and formatted. The final version may differ from this version.

Introduction

G-protein-coupled receptors (GPCRs) form a large and functionally diverse superfamily which represents ~1-2 % of encoded genes in the human genome. Despite being activated by a wide variety of stimuli from photons to glycoproteins (Kristiansen, 2004), these receptors exhibit primary sequence homology and a conserved tertiary structure comprising a bundle of seven transmembrane (TM) domains. Although much is known about some of the structural features involved in the binding of ligands, the actual mechanism for ligand activation is less well defined. Agonist occupancy of GPCRs is believed to result in conformation changes which lead to activation of specific G-proteins (Karnik, 2003; Wong, 2003). Studies with mutant GPCRs suggest that intracellular loops (particularly second and third) and the cytoplasmic C-terminus provide important epitopes for a number of signaling and regulatory proteins including G-proteins, arrestins and G-protein-receptor kinases (Wong, 2003; Tan et al., 2004). One highly conserved triplet of amino-acids (Asp-Arg-Tyr) is located at the interface of TM-III and second intracellular loop (IC2) in class I "rhodopsin-like" GPCRs (Fig. 1). This "DRY" motif has been described to provide a pivotal role in signal transduction of GPCRs. The aspartate (or glutamate in rhodopsin) has been reported to be important for stabilizing intramolecular interactions, notably with the neighboring arginine, thereby constraining GPCRs in the inactive (R) conformation. Mutation of this Asp/Glu disrupts this constraint and has resulted in ability of some GPCRs to adopt an active conformation (R*) state (Scheer et al., 1996; Scheer et al., 1997). This conformational change is hypothesized to reposition the arginine from a polar pocket and is considered to be important for interaction with G-proteins (Ballesteros et al., 1998; Scheer et al., 2000).

Molecular Pharmacology Fast Forward. Published on July 27, 2005 as DOI: 10.1124/mol.105.013359
This article has not been copyedited and formatted. The final version may differ from this version.

Mutagenesis studies in a number of receptors have demonstrated the importance of this arginine, including the well documented α_{1b}-adrenergic receptor (AR) (Scheer et al., 2000), which showed increased agonist-binding affinities but impaired receptor signaling by decreasing its ability to couple to G-proteins. In other receptors, mutation has resulted in impaired receptor signaling with decreases in agonist-binding (e.g. Capra et al., 2004; Chung et al., 2002; Jones et al., 1995). Naturally occurring mutations have been identified which result in receptor dysfunction and responsible for certain diseases (e.g. nephrogenic diabetes insipidus (NDI) (Morello and Bichet, 2001) and hypogonadotropic hypogonadism (Costa et al., 2001)). The significance of the aspartate has been studied and has resulted in constitutive activity for some receptors (e.g. histamine H_2 receptor (H_2R), Alewijnse et al., 2000; α_{1b}-AR, Scheer et al., 1997 and β_2-AR, Rasmussen et al., 1999) but not in others, where only effects on receptor expression were reported (e.g. m1 muscarinic receptors (mAChR); Lu et al., 1997). The tyrosine residue is the least conserved and studied amongst this triad sequence, with cysteinyl, histidyl and serine residues occurring in some GPCRs such as oxytocin (OT), V_2 vasopressin (AVP) and gonadotropic releasing hormone (GnRH) receptors respectively. Collectively, these observations have given rise to the possibility that the DRY motif may not have the same function in all GPCRs.

The neurohypophysial hormones AVP and OT are structurally-related nonapeptides, which mediate a plethora of physiological functions, including vasopressor and antidiuretic actions, by binding to specific receptors (Gimpl and Fahrenholz, 2001; Thibonnier et al., 2001a). At present, four AVP/OT receptor subtypes ($V_{1a}R$, $V_{1b}R$, V_2R and OTR) have been cloned from different species and constitute a sub-family of the larger GPCR superfamily which possess

discrete, but related pharmacological profiles. The $V_{1a}R$ is widely expressed and mediates nearly all of the actions of AVP with the exception of antidiuresis (renal V_2R) and adrenocorticotropic hormone secretion (pituitary $V_{1b}R$). AVP mediates vascular smooth muscle ($V_{1a}Rs$) contraction and regulate cardiovascular function (Thibonnier et al., 2001a). In contrast, OT results in contraction of uterine myometrium (OTRs) during labour and mammary myoepithelium to elicit lactaction (Gimpl and Fahrenholz, 2001). With the exception of the V_2R (which couples to adenylyl cyclase), these receptors couple to $G\alpha_{q/11}$ thereby generating inositol 1,4,5 trisphosphate ($InsP_3$) and diacylglycerol as second messengers. Currently, identification of domain(s) involved in G-protein coupling and in receptor activation has been limited. The importance of the IC2 region in $G\alpha_{q/11}$ coupling (Liu and Wess, 1996) and C-terminus for the $V_{1a}R$ has been proposed (Hawtin et al., 2001; Thibonnier et al., 2001b). However, the functional significance of the highly conserved DRY motif for the $V_{1a}R$ has not yet been determined. The aims of the present study were to examine the functional consequences of inserting conservative and non-conservative mutations in this motif for the $V_{1a}R$.

Molecular Pharmacology Fast Forward. Published on July 27, 2005 as DOI: 10.1124/mol.105.013359
This article has not been copyedited and formatted. The final version may differ from this version.

Materials and Methods

Materials. The cyclic antagonist 1-(β-mercapto-β,β-cyclopentamethylene propionic acid), 2-(O-methyl)tyrosine AVP (CA) was purchased from Bachem (UK). AVP and the linear antagonist phenyl acetyl-*D*-Tyr(Me)^{2}Arg^{6}Tyr(NH$_2$)^{9}AVP (LA) were from Sigma (Poole, UK). (2S)-[(2R 3S)-(5-chloro-3-(2-chlorophenyl)-1-(3,4-dimethoxybenzene-sulfonyl)-3-hydroxy-2,3-dihydro-1H-indole-2-carbonyl]-pyrrolidine-2-carboxamide (SR 49059) was obtained from Sanofi Recherche (Toulouse, France). Cell culture media and supplements were purchased from Gibco (Uxbridge, UK). Modifying enzymes including *BspT*I and *BshT*I were obtained from MBI Fermentas (Sunderland, UK). All other reagents were of analytic grade and obtained from various commercial suppliers.

Mutant receptor constructs. Mutation of the V_{1a}R was made using a PCR approach as described previously (Hawtin et al., 2002). The wild-type rat V_{1a}R was modified to contain a unique *Bsh*TI restriction site (underlined) using the primer 5'-G-ACA-GCC-GAC-CG**G**-TAC-ATC-GCC-GTG-TGC-3' containing the appropriate base change without affecting the coding sequence (bold). The PCR product was subcloned (*Hind*III and *Kpn*I) into the mammalian expression vector pcDNA3 containing a previously engineered hemagglutinin (HA)-epitope tag incorporated after the initiation methionine in the amino-terminus of the wild-type V_{1a}R sequence (Hawtin et al., 1997). This construct was further modified by incorporating a single base change (bold) for a unique *Bsp*TI restriction site (underlined) using the primer 5'-GCC-GAC-CGG-TAC-ATC-GCC-GTG-TGC-CAC-CCG-CTT-AAG-ACC-3'. A *Bsh*TI/ *Kpn*I product was subcloned into the pcDNA3 construct above to give pcDNA3-[*Bsh*TI/*Bsp*TI]V_{1a}R.

Molecular Pharmacology Fast Forward. Published on July 27, 2005 as DOI: 10.1124/mol.105.013359
This article has not been copyedited and formatted. The final version may differ from this version.

The mutant constructs [D148A]V_{1a}R, [R149A]V_{1a}R, [Y150A]V_{1a}R, [D148E]V_{1a}R, [D148N]V_{1a}R, [D148R]V_{1a}R, [R149D]V_{1a}R, [R149H]V_{1a}R and [D148R/R149D]V_{1a}R were made using the following antisense oligonucleotides: 5'-G-GGT-CTT-AAG-CGG-GTG-GCA-CAC-GGC-GAT-GTA-CCG-G**G**C-GGC-TGT-CAT-C-3'; 5'-G-GGT-CTT-AAG-CGG-GTG-GCA-CAC-GGC-GAT-GTA-C**GC**-GTC-GGC-TGT-C-3'; 5'- G-GGT-CTT-AAG-CGG-GTG-GCA-CAC-GGC-GAT-G**GC**-CCG-GTC-GG-3'; 5'-G-GGT-CTT-AAG-CGG-GTG-GCA-CAC-GGC-GAT-GTA-CCG-**T**TC-GGC-TGT-CAT-C-3', 5'-G-GGT-CTT-AAG-CGG-GTG-GCA-CAC-GGC-GAT-GTA-CCG-GT**T**-GGC-TGT-CAT-C-3', 5'-G-GGT-CTT-AAG-CGG-GTG-GCA-CAC-GGC-GAT-GTA-CCG-G**CG**-GGC-TGT-CAT-C-3', 5'-G-GGT-CTT-AAG-CGG-GTG-GCA-CAC-GGC-GAT-GTA-**GTC**-GTC-GGC-TGT-C-3', 5'-G-GGT-CTT-AAG-CGG-GTG-GCA-CAC-GGC-GAT-GTA-**AT**G-GTC-GGC-TGT-C-3' and 5'-G-GGT-CTT-AAG-CGG-GTG-GCA-CAC-GGC-GAT-GTA-**GTC**-G**CG**-GGC-TGT-C-3' respectively and using [*Bsh*TI/*Bsp*TI]V_{1a}R-pcDNA3 as template. Each primer contained the unique *Bsp*TI restriction site (underlined) and appropriate base changes (bold) to introduce specific mutation(s) at the desired location within the HA-tagged V_{1a}R coding sequence. Each PCR product was subcloned into pcDNA3-[*Bsh*TI/*Bsp*TI]V_{1a}R utilizing *Hind*III and *Bsp*TI restriction sites. All receptor constructs were confirmed by automated fluorescent sequencing (University of Nottingham, UK).

Cell culture and transfection. Human embryonic kidney (HEK) 293T cells were routinely cultured in Dulbecco's modified Eagles medium (DMEM) supplemented with 10 % (v/v) fetal calf serum (FCS) in humidified 5 % (v/v) CO_2 in air at 37 °C. Cells were seeded at a density

Molecular Pharmacology Fast Forward. Published on July 27, 2005 as DOI: 10.1124/mol.105.013359
This article has not been copyedited and formatted. The final version may differ from this version.

of approximately 5 x 10^5 cells/100 mm dish and transfected after 48 h using a calcium phosphate precipitation protocol with 10 μg DNA/dish.

Radioligand binding assays. A washed cell membrane preparation of HEK 293T cells was prepared 36 hr post-transfection as previously described (Hawtin et al., 2002) and the protein concentration determined using the BCA protein assay kit (Sigma) with BSA as standard. Competition radioligand binding assays were performed in MultiScreen™ HTS 96-well opaque plates (Millipore, Watford, UK) containing 1.0 μm glass fiber (GF/B) filters and using the natural agonist [Phe^3-3,4,5-^{3}H]AVP, (73 Ci/mmol; Perkin-Elmer, Groningen, Netherlands) as tracer ligand. Radioligand binding assays were performed in binding buffer (20 mM HEPES, 10 mM $Mg(CH_3COO_2)_2$ and 1 mM EGTA; pH 7.4) and supplemented with 0.05 % (w/v) BSA. Each well (final volume of 250 μl) contained radioligand (0.4 – 2.4 nM), cell membranes (100 - 330 μg) and competing ligand (at the concentrations indicated) and incubated at 25 °C for 90 min to establish equilibrium. Non-specific binding was determined in parallel incubations using 10 μM unlabelled AVP as appropriate. Bound radioligand was separated from free ligand by filtration using a vacuum manifold system (Millipore). Filters were washed twice with ice-cold binding buffer without BSA and sealed with opaque backing tape. Following the addition of MicroScint-20 (Perkin-Elmer), radioactivity was measured using a Topcount NXT scintillation counter (Perkin-Elmer). Binding data were analyzed by non-linear regression to fit theoretical Langmuir binding isotherms to the experimental data using Prism4 software (GraphPad Software Inc., San Diego, CA). Individual IC_{50} values obtained for competing ligands were corrected for radioligand occupancy as described (Cheng

Molecular Pharmacology Fast Forward. Published on July 27, 2005 as DOI: 10.1124/mol.105.013359
This article has not been copyedited and formatted. The final version may differ from this version.

and Prusoff, 1973) using the radioligand affinity (K_i) experimentally determined for each construct.

AVP-induced inositol phosphate production. HEK 293T cells were seeded at a density of 7.5 x 10^4 cells/well in poly *D*-lysine-coated 24 well plates and transfected with cDNA (0.5 μg/well) after 24 h using Transfast™ (Promega Corp., Southampton, UK) as described in the manufacturer's protocol. The assay for AVP-induced accumulation of inositol phosphates (InsPs) was based on that described previously (Hawtin et al., 2002). Essentially, 16 h post-transfection, medium was replaced with inositol-free DMEM (Gibco) containing 1 % (v/v) FCS and 1 μCi/ml myo-[2-^{3}H]inositol (20.0 Ci/mmol; MP Biomedicals, Irvine, CA) for 24 h. Cells were washed twice with PBS, then incubated in inositol-free media containing 10 mM LiCl for 30 min, after which AVP was added at the concentrations indicated for a further 30 min. Incubations were terminated by addition of ice-cold 0.1 M HCOOH for 30 min. Samples were loaded onto Bio-Rad AG1-X8 columns (formate form) and diluted in 10 ml of water. Following the elution of inositol and glycerophosphoinositol (10 ml of 25 mM NH_4COOH containing 0.1 M HCOOH), a mixed inositol fraction containing mono-, bis-, and trisphosphates (InsP – $InsP_3$) was eluted with 5 ml of 850 mM NH_4COOH containing 0.1 M HCOOH, mixed with UltimaFlo AF scintillation cocktail (Perkin-Elmer) and radioactivity quantified by liquid scintillation spectroscopy. EC_{50} values were determined by non-linear regression after fitting of logistic sigmoidal curves to the experimental data.

Cell surface expression of mutant receptors. Cell surface expression of mutant $V_{1a}R$ constructs was determined by using an indirect ELISA based method. Briefly, HEK 293T cells

Molecular Pharmacology Fast Forward. Published on July 27, 2005 as DOI: 10.1124/mol.105.013359
This article has not been copyedited and formatted. The final version may differ from this version.

were seeded at a density of 7.5 x 10^4 cells/well in poly *D*-lysine-coated 24-well plates and transfected as described above. After 36 h, cells were fixed with 3.7 % (v/v) formaldehyde in TBS (20 mM TRIS, 150 mM NaCl; pH 7.5) for 15 min at 25 °C. Cells were washed three times with TBS. Non-specific binding was blocked with 3 % (w/v) BSA in TBS for 45 min. The anti-HA primary antibody (HA-7; Sigma) was diluted to 1:30,000 in 3 % (w/v) BSA/TBS prior to the addition to each well for 60 min at room temperature with occasional shaking, followed by three gentle washes with TBS. Cells were briefly reblocked with 3 % (w/v) BSA in TBS for 15 min, prior to incubation with secondary goat anti-mouse conjugated alkaline phosphatase (Sigma) diluted to 1:20,000 in 3 % (w/v) BSA/TBS for 60 min with occasional shaking. Cells were washed three times with TBS, prior to the addition of 250 µl of the colorimetric alkaline phosphate substrate *p*-nitrophenol phosphate (5 mM) dissolved in diethanolamine buffer (1 M diethanolamine, 280 mM NaCl, 0.5 mM $MgCl_2$; pH 9.4) to each well. Plates were incubated at 37 °C until an adequate color change had occurred (45 min), at which time a 100 µl sample was taken, mixed with an equal volume of 0.4 M NaOH prior to colorimetric reading at 405 nm using a Dynatech Laboratories MRX plate reader. For each experiment, mock conditions corresponding to the transfection of vector without receptor were included. The percentage of mutant receptor expressed at the cell surface is defined as 100 x $[(OD_{mutant} - OD_{mock})/(OD_{wt} - OD_{mock})]$. All experiments were performed in triplicate for each condition and values were obtained from at least three separate experiments.

Agonist-mediated internalization of mutant receptors. HEK 293T cells were seeded in 24-well plates and transfected with receptor mutant cDNA using Transfast™ as described above. After 36 h, media from cells was replaced with fresh pre-warmed growth media. To promote

Molecular Pharmacology Fast Forward. Published on July 27, 2005 as DOI: 10.1124/mol.105.013359
This article has not been copyedited and formatted. The final version may differ from this version.

$V_{1a}R$ internalization, cells were exposed to AVP for different time intervals over a maximum period of 60 min at 37 °C with 5 % (v/v) CO_2 in air. Cells were fixed and quantification of receptor's remaining at the cell surface was determined using the ELISA-based assay as described above. The percentage of mutant receptor internalized is defined as 100 x $[(OD_{basal} - OD_{mock}) - (OD_{stimulated} - OD_{mock})]/(OD_{basal} - OD_{mock})$. All experiments were performed in triplicate for each condition and values from at least three separate experiments.

Immunohistocytochemistry. HEK 293T cells were seeded in 24-well plates containing poly *D*-lysine-coated glass cover slips (12 mm) and transfected using Transfast™ as described above. Cells were fixed and washed with TBS as described previously for the ELISA. Cells were blocked with 3 % (w/v) BSA/TBS containing glycine (1 % (w/v)) for 45 min, followed by incubation with anti-HA primary antibody (diluted to 1:3,000 in 3 % (w/v) BSA/glycine/TBS for 60 min. Cells were washed three times with TBS prior to reblocking with 10 % (v/v) goat serum in PBS for 15 min at room temperature. Cells were labeled with secondary antibody goat anti-mouse Rhodamine Red X (Molecular Probes, Leiden, The Netherlands) (diluted to 1:500 in 10 % (v/v) goat serum in PBS) for 60 min at room temperature in the dark. After a further three washes cover slips were mounted on glass slides prior to confocal microscopy.

Confocal microscopy. Confocal microscopy was performed using a Zeiss LSM 510 laser scanning microscope with a Zeiss Plan-Apo 63x 1.4 NA oil immersion objective. The HA-tagged receptors were visualized by exciting the rhodamine red-X secondary antibody with a 543 nm HeNe laser and a 560 nm long pass filter. For each slide, images were captured at

random sites from three separate experiments. The gains and offsets were kept constant for each image that was generated using the Zeiss LSM software (Jena, Germany).

Molecular Pharmacology Fast Forward. Published on July 27, 2005 as DOI: 10.1124/mol.105.013359
This article has not been copyedited and formatted. The final version may differ from this version.

Results

Pharmacological characterization of alanyl-substituted "DRY" mutant $V_{1a}R$ constructs

The aim of this study was to establish if the highly conserved "DRY" motif is important for ligand binding, signaling and agonist-mediated internalization of receptors. Based on the crystal structure of rhodopsin (Palczewski et al., 2000), the "DRY" motif is embedded within TM3 at the interface of the IC2 region (Fig. 1). Indeed, the Arg^{149} within this motif (i.e. Arg(3.50), using nomenclature proposed by Ballesteros and Weinstein (1995)) is one of the most conserved residues in GPCRs. All members of the neurohypophysial peptide hormone receptor family cloned to-date have an aspartyl (3.49) and arginyl (3.50) at these loci (Fig. 1). In contrast, the residue at position 3.51 is less conserved within this family. A histidyl residue is found only in V_2Rs, with cysteines present for all species of OTRs. In the case of V_{1a}Rs and V_{1b}Rs, a tyrosine residue is absolutely conserved (Fig. 1).

To identify the contribution to ligand binding provided by individual residues within this "DRY" motif, residues Asp^{148}, Arg^{149} and Tyr^{150} of the V_{1a}R were individually mutated to alanine to give [D148A]V_{1a}R, [R149A]V_{1a}R and [Y150A]V_{1a}R respectively. Each mutant receptor construct was expressed in HEK 293T cells and their pharmacological characteristics compared to a HA-tagged wild-type (Wt) V_{1a}R. Incorporation of the HA-epitope sequence at the amino-terminus was previously shown not affect ligand binding or signaling compared to an untagged Wt V_{1a}R (Hawtin et al., 1997) and was used in all subsequent experiments. Pharmacological characterization was aided by the fact that four different classes of ligand are available for probing changes in the ligand binding profile of V_{1a}R constructs. In each case,

Molecular Pharmacology Fast Forward. Published on July 27, 2005 as DOI: 10.1124/mol.105.013359
This article has not been copyedited and formatted. The final version may differ from this version.

competition radioligand binding curves were determined using a recently developed 96-well filtration assay with the natural agonist AVP and three different structural classes of antagonist: (i) cyclic peptide antagonist ($d(CH_2)_5Tyr(Me)^2AVP$, (Kruszynski et al., 1980)) containing a twenty-membered ring formed by a disulfide bond between Cys^1 and Cys^6; (ii) linear peptide antagonist ([PhAc*D*-$Tyr(Me)^2Arg^6Tyr(NH_2)^9$]AVP, (Schmidt et al., 1991)) and (iii), non-peptide antagonist (SR 49059; (Serradeil-Le Gal, C. et al., 1993)). The K_i values are presented in Table 1, corrected for radioligand occupancy. The mutant constructs [R149A]$V_{1a}R$ and [Y150A]$V_{1a}R$, exhibited a pharmacological profile very similar to Wt, although the K_i for AVP and the three different classes of antagonist was slightly raised (2-6 fold) in each case (Table 1). In marked contrast, [D148A]$V_{1a}R$ was unable to bind tracer ligand. With the exception of [D148A]$V_{1a}R$, Wt and remaining mutant constructs were all expressed at approximately the same level of 1-2 pmol/mg protein.

The capability of each of the mutant receptor constructs to generate an intracellular signal in response to the natural agonist AVP was also investigated. In each case, AVP-induced accumulation of InsPs was assayed (Fig. 2A). From the resulting dose-response curves, the EC_{50} and E_{max} were determined for each construct and these are presented in Fig. 2B. The EC_{50} value for [R149A]$V_{1a}R$ and [Y150A]$V_{1a}R$ was slightly higher than the Wt receptor in each case, reflecting the slight decrease in affinity of AVP at these constructs (Table 1). In the case of [D148A]$V_{1a}R$, this mutant failed to signal even when challenged with high concentrations (10 μM) of AVP (Fig. 2B). Furthermore, the E_{max} for all mutant constructs was at least 50 % lower than Wt (Fig. 2B). It is also noteworthy that the basal level of InsPs accumulation was not significantly different (using ANOVA with a post hoc Dunnett's test

Molecular Pharmacology Fast Forward. Published on July 27, 2005 as DOI: 10.1124/mol.105.013359
This article has not been copyedited and formatted. The final version may differ from this version.

analysis (GraphPad Prism4) between each of the mutants and Wt, an indication that none of the mutants displayed an enhanced level of constitutive activity. Consequently, the disruption of ligand binding and intracellular signaling of [D148A]V_{1a}R may be due to this mutant failing to be trafficked efficiently to the plasma membrane.

Mutation of Asp^{148} resulted in impaired cell surface receptor expression

The mutant receptors [D148A]V_{1a}R, [R149A]V_{1a}R and [Y150A]V_{1a}R each contained the HA-epitope tag incorporated at their N-terminus (Fig. 1). An ELISA-based assay was developed to quantify expression of mutant receptors at the cell-surface compared to HA-tagged Wt expression. This technique offers considerable advantages compared to other techniques (e.g. whole cell binding) as this doesn't rely on the binding interaction of a tracer ligand which may or may not be altered with a specific mutation. Furthermore, this technique allows more accurate quantification of receptors at the cell surface to be assessed by direct comparison to other receptors in parallel experiments compared to microscopy. To validate that the ELISA was measuring cell surface expression we compared the cell surface localization of HA-tagged Wt V_{1a}R and a mock transfected vector using immunofluorescence confocal microscopy (Fig. 3). The transfected control vector gave no background signal (Fig. 3AB). In contrast, the Wt V_{1a}R was clearly shown to be expressed at high levels on the cell surface (Fig. 3CD) and confirmed that the ELISA technique provides a high-signal to noise ratio for quantification of cell surface receptors.

The mutant constructs [R149A]V_{1a}R and [Y150A]V_{1a}R were all expressed on the cell surface at levels similar to Wt determined by ELISA (Table 1). In contrast, [D148A]V_{1a}R was not

Molecular Pharmacology Fast Forward. Published on July 27, 2005 as DOI: 10.1124/mol.105.013359
This article has not been copyedited and formatted. The final version may differ from this version.

expressed on the cell surface shown by ELISA (Table 1) or with confocal microscopy (Fig. 3EF). Permeabilization of the cell membrane with 0.1 % (v/v) Triton X-100 prior to quantification of receptor, revealed that the mutant [D148A]V_{1a}R was actually expressed at low levels, but was retained inside the cell (data not shown, Fig. 3D). Furthermore, we also tested whether increasing the cDNA during transfection (0.125-2.0 μg/well) was able to increase cell-surface expression or signaling of the [D148A]V_{1a}R mutant. However, cell surface expression or inositol phosphate signaling was not increased above levels shown in Table 1 and 2 (data not shown). These results show that Asp^{148} is critical for trafficking and/or delivery of the V_{1a}R to the cell surface.

Agonist-mediated internalization of wild-type and V_{1a}R mutants $Ala^{149}$and Ala^{150}

Most GPCRs are internalized in response to prolonged agonist stimulation. For V_{1a}Rs, these are internalized via a β-arrestin-dependent pathway (Bowen-Pidgeon et al., 2001) and are both agonist-, and time-dependent (Fig 4A). Indeed as little as 1 nM AVP is able to promote internalization of ~30 % of receptors over a 60 min period (data not shown). To evaluate if Arg^{149} and/or Tyr^{150} provide important epitope(s) for AVP-mediated V_{1a}R internalization, we compared the mutations engineered at these sites to the internalization kinetics of Wt receptors using the ELISA-based assay. Using HEK 293T cells transiently expressing Wt V_{1a}R, [R149A]V_{1a}R and [Y150A]V_{1a}R at equivalent abundance, it was found that AVP (1 μM) promoted internalization of all receptors (Fig. 4A). After exposure to AVP for 60 min, the percentage of cell surface receptors internalized (~60 %) was the same in each case (Fig. 4B). Furthermore, the rate of internalisation (time for 50 % of receptors that are sensitive to

Molecular Pharmacology Fast Forward. Published on July 27, 2005 as DOI: 10.1124/mol.105.013359
This article has not been copyedited and formatted. The final version may differ from this version.

internalization) was not significantly different compared to Wt $V_{1a}R$ using ANOVA with a post hoc Dunnett's test analysis (GraphPad Prism4) (Fig. 4B).

Specific requirements at position-148 for cell surface delivery and functional recovery

To evaluate the properties of the Asp^{148} residue that underlie its importance for $V_{1a}R$ cell surface expression and function, the constructs [D148N]$V_{1a}R$, [D148E]$V_{1a}R$ and [D148R]$V_{1a}R$ were engineered. These mutant receptors probed the importance of the charge of Asp^{148}, by (i) removing the charge but still maintaining the overall side chain length ([D148N]$V_{1a}R$), (ii) preserving the negative charge ([D148E]$V_{1a}R$) whilst extending the side-chain length with an additional methylene or (iii), substitution with a positively charged residue [D148R]$V_{1a}R$. The [D148R]$V_{1a}R$ was not detected on the cell surface (Table 2), whereas both [D148N]$V_{1a}R$ and [D148E]$V_{1a}R$ mutants showed a significant increase in cell surface expression compared to [D148A]$V_{1a}R$ (Fig. 5A). However, their cell surface expression was reduced to ~20 % ([D148N]$V_{1a}R$) and ~40 % ([D148E]$V_{1a}R$) of normal Wt levels and this was identical at 24 h (data not shown) and 36 h post-transfection (Fig 5A; Table 2). It was important to ascertain if recovery of cell surface expression with these mutants was a necessary prerequisite for restoration of ligand binding and signaling that was absent for [D148A]$V_{1a}R$ (Table 1). Although the [D148N]$V_{1a}R$ mutant showed an increased surface expression compared to [D148A]$V_{1a}R$, it was unable to bind [^{3}H]AVP tracer ligand (Table 2) or signal in response to AVP (10 μM) challenge (Fig. 6C). Similarly, [D148R]$V_{1a}R$ was unable to bind tracer (Table 2) or signal (Fig. 6C). In contrast, the [D148E]$V_{1a}R$ mutant was able to bind both agonist and antagonist ligands and exhibited a pharmacological profile very similar to Wt (Table 2), although the K_i for AVP was slightly raised ~5-fold. The ability of [D148E]$V_{1a}R$ to generate

Molecular Pharmacology Fast Forward. Published on July 27, 2005 as DOI: 10.1124/mol.105.013359
This article has not been copyedited and formatted. The final version may differ from this version.

an intracellular signal was also assessed (Fig. 6A). From the resulting dose-response curve, the EC_{50} value for [D148E]V_{1a}R was almost identical to Wt receptor, despite having a reduced E_{max} (Fig. 6C). Basal level of InsPs signaling was not significantly increased (ANOVA with a post hoc Dunnett's test analysis (GraphPad Prism4) in both mutants relative to Wt (data not shown). Collectively, these results show the importance of a negative charge at position-148 for cell surface delivery and subsequent restoration of ligand binding and V_{1a}R signaling capacity.

Conservative mutation of Glu^{148} displayed enhanced receptor internalization

Following the recovery of cell surface expression with [D148E]V_{1a}R, it now allowed us to probe if this conservative substitution at position-148 was important for AVP-mediated V_{1a}R internalization. As described previously, the internalization kinetics of [D148E]V_{1a}R was compared to Wt V_{1a}Rs using the ELISA-based assay. After exposure to AVP for 60 min, the percentage of cell surface receptors present at the cell surface was able to be internalized was significantly increased (~80 %) for [D148E]V_{1a}R compared to ~60 % for Wt receptor (Fig. 7A). However, the rate at which this mutant receptor was internalized ($t_{1/2}$ ~ 7 min) was very similar to Wt (Fig. 7C).

Charge specific requirements at position-149 for surface expression and normal V_{1a}R function

The observation that a negatively charged residue was important at position-148, raised the possibility that charged residues within this TM-III-IC2 interface may have a wider importance in cell surface delivery and also raised the possibility of a mutual interaction between Asp^{148}

Molecular Pharmacology Fast Forward. Published on July 27, 2005 as DOI: 10.1124/mol.105.013359
This article has not been copyedited and formatted. The final version may differ from this version.

and Arg^{149}. To evaluate this, we engineered the constructs [R149D]V_{1a}R, [R149H]V_{1a}R and [D148R/R149D]V_{1a}R. These mutant receptors probed the importance of Arg^{149}, by (i) reversing the charge with substitution of an aspartyl (i.e. [R149D]V_{1a}R), (ii) preserving the positive charge with a histidyl (i.e. [R149H]V_{1a}R) or (iii), switching the charged residues at positions-148 and 149 respectively (i.e. [D148R/R149D]V_{1a}R). The mutants [R149D]V_{1a}R and [D148R/R149D]V_{1a}R were not expressed on the cell surface determined by ELISA (Fig. 5B; Table 2) or confocal microscopy (data not shown). Consequently, these mutants were unable to bind tracer ligand (Table 2) or signal when challenged with AVP (10 μM; Fig. 6C). In contrast, the [R149H]V_{1a}R mutant was expressed on the cell surface. However, this was consistently reduced to ~60 % of Wt surface expression levels (Fig 5B; Table 2). This [R149H]V_{1a}R mutant was able to bind both agonist and antagonist ligands and exhibited a pharmacological profile comparable to wild-type (Table 2), although the K_i for AVP was slightly higher (~4-fold) which was also observed for [R149A]V_{1a}R (Table 1). The ability of [R149H]V_{1a}R to increase second messenger generation was assessed (Fig. 6B). The dose-response curves for AVP-induced accumulation of InsPs for [R149H]V_{1a}R and [R149A]V_{1a}R (Fig. 2A) was equally right-shifted compared to Wt, with EC_{50} values increasing by approximately ~3-fold (Fig. 6C), and reflecting the slight decrease in affinity of AVP for both of these constructs (Table 1 and 2). The basal level of InsPs signaling for all mutants was not increased relative to Wt V_{1a}R using ANOVA with a post hoc Dunnett's test analysis (GraphPad Prism4) (data not shown).

Rapid internalization kinetics of a conservative His^{149} mutation

An inherited mutation in the related V_2R ([R137H]V_2R) is found in some patients suffering with the disease NDI, a condition which results in their inability to retain water in the kidney (Morello and Bichet, 2001). Pharmacological assessment of [R137H]V_2R in recombinant cells showed this mutant failed to response to AVP, by having a reduced cell surface expression and intracellular localization of receptors (Barak et al., 2001). This subsequently resulted in the phenomenon of some mutations being described as constitutively internalized (Wilbanks et al., 2002). The analogous substitution in the $V_{1a}R$ (i.e. [R149H]$V_{1a}R$) showed a ~40 % reduced cell surface expression, but was expressed at sufficient levels to perform internalization experiments. Agonist-mediated internalization of [R149H]$V_{1a}R$ was compared in parallel to Wt $V_{1a}Rs$. After exposure to AVP stimulation for 60 min, the percentage of cell surface receptors that was internalized was increased for [R149H]$V_{1a}R$ (~70 %) relative to Wt (Fig. 7B). Interestingly, the rate at which this mutant receptor was internalized ($t_{1/2}$ ~ 4 min) was significantly increased compared to Wt (Fig. 7C).

Molecular Pharmacology Fast Forward. Published on July 27, 2005 as DOI: 10.1124/mol.105.013359
This article has not been copyedited and formatted. The final version may differ from this version.

Discussion

In this report, site-directed mutagenesis of the $V_{1a}R$ was used to study the role of the conserved DRY motif located at the cytosolic end of TM-III (Fig. 1). Mutation of the conserved aspartyl (3.49) residue ([D148A]$V_{1a}R$) resulted in a receptor that was not expressed on the cell surface and consequently unable to bind tracer ligand or increase AVP-mediated InsP signaling. Despite the lack of surface expression, this mutant was localized within intracellular compartments following permeabilization. However, these levels were still below detectable limits to establish specific-binding in membrane samples. A similar situation has been reported for other members of AVP/OT receptor family. For example, replacement of Asp^{136} (Asp(3.49)) with an alanyl in the OTR also displayed reduced expression (Fanelli et al., 1999). This mutant was unable to bind [^{3}H]OT tracer or increase OT-mediated InsP production. This phenomenon of reduced expression (usually <10 % of Wt) has been observed in other Asp(3.49) mutant receptors such as H_2R (Alewijnse et al., 2000), m1 mAChR (Lu et al., 1997), V_2R (Morin et al., 1998) and GnRH receptors (Arora et al., 1997). The reasons for this impaired expression at this locus is not yet clear, however, reduction in receptor stability, mis-folding and receptor desensitization and internalization have been proposed (Wilbanks et al., 2002).

One possibility for the lack of [D148A]$V_{1a}R$ surface expression could be explained by the receptor being down-regulated as a consequence of constitutive activity. This mutant did not display any increased basal signaling activity (indication of constitutively activity). In some studies involving mutation of Asp(3.49), any subsequent low expression has often been normalized or the amount of cDNA transfected increased to allow direct comparison of

Molecular Pharmacology Fast Forward. Published on July 27, 2005 as DOI: 10.1124/mol.105.013359
This article has not been copyedited and formatted. The final version may differ from this version.

equivalent Wt expression. Increasing the cDNA of [D148A]V_{1a}R did not further increase surface expression or signaling. It is important to note that this approach must be taken with caution as a proportion of the receptor may be localized intracellularly. GPCRs are considered to undergo a basal level of endogenous synthesis/re-cycling (Parnot et al., 2002; Milligan, 2003). Accumulation or increased levels of intracellular receptors may alter this equilibrium and induce a degree of constitutive activity as an artifact of adjusting expression levels using values determined by binding. Indeed, Wt receptors can adopt an enhanced constitutive active profile following over-expression. Moreover, translocation of intracellular localized H_2Rs to the cell surface can be dramatically increased with inverse agonists (Smit et al., 1996).

To probe the importance of Asp^{148} that is crucial for surface delivery, mutants which removed ([D148N]V_{1a}R), preserved ([D148E]V_{1a}R) or reversed this charge ([D148R]V_{1a}R) were engineered. The [D148N]V_{1a}R and [D148R]V_{1a}R mutants were expressed at too low levels to detect significant specific-binding and signaling. In contrast, the glutamyl substitution was able to bind ligands and signal, albeit with a reduced maximal coupling ability. This implies that the negative charge at Asp(3.49) is, or at least in part, important for increasing cell-surface delivery and subsequent restoration of normal V_{1a}R function. A similar scenario was observed for D130E/N mutations in eotaxin CCR3 receptors (Auger et al., 2002). The importance of side-chain substitutions at Asp(3.49) have been extensively studied in m1 mAChRs which severely reduce expression levels (Lu et al., 1997). In contrast, replacement of Asp^{142} in α_{1b}-ARs with all possible 19 encoding amino-acids, revealed the importance of side-chains for influencing the degree of constitutive activity (Scheer et al., 1997). If a mutant is constitutively active then an increase in agonist-binding affinity, elevated basal and potency for

Molecular Pharmacology Fast Forward. Published on July 27, 2005 as DOI: 10.1124/mol.105.013359
This article has not been copyedited and formatted. The final version may differ from this version.

second-messenger generation is often observed as a result of mimicking the active conformation (R*) of a receptor. For [D148E]V_{1a}R, agonist-binding affinity was in fact the opposite with a slight ~4-fold reduction, suggesting that the glutamyl is exerting a subtle conformational change only required for agonist-binding. This occurred without increasing basal signaling activity.

Another reason for the loss of surface expression with Asp^{148} mutations may be related to their structural instability within the receptor architecture. The mutants may display differential retention within the ER and/or insertion into the plasma membrane. This may render the receptor more susceptible to degradation and/or internalization once trafficked to the membrane. Only [D148E]V_{1a}R was expressed at sufficient levels to investigate changes in internalization. Once delivered to the surface, a greater proportion of [D148E]V_{1a}R was internalized compared to Wt without affecting the rate. Interestingly, a similar situation was observed for D136E/N mutations in GnRH receptors (Arora et al., 1997). This enhanced level of internalization or degradation may contribute to reduced expression for other Asp(3.49) mutant GPCRs. Indeed, mutant GPCRs that have been described as constitutively active e.g. H_2R (Alewijnse et al., 2000) and β_2-AR (Rasmussen et al., 1999) have reported structural instabilities. The role of Asp(3.49) for V_{1a}Rs does not belong to the subgroup of GPCRs that when mutated result in constitutive activity. Instead, they have properties similar to those described for m1 mAChR (Lu et al., 1997), α_{2a}-AR (Chung et al., 2002) and GnRH receptors (Arora et al., 1997).

Molecular Pharmacology Fast Forward. Published on July 27, 2005 as DOI: 10.1124/mol.105.013359
This article has not been copyedited and formatted. The final version may differ from this version.

The region of the DRY motif has been modeled by Scheer et al., (2000) and suggests that the arginine is embedded within the receptor in the inactive state. Upon ligand-mediated receptor activation, the conformation change results in the movement of the arginine side-chain to the cytoplasmic surface. This suggests that exposure of the arginine is a crucial event in G-protein binding and/or activation. These results do not fully support this general hypothesis as the alanyl substitution was able to bind agonist, signal and internalized as normal. Although this mutant did show a reduced maximal signaling ability. This reduction-of-function phenotype may be caused by the uncoupling of V_{1a}Rs from the G-protein, but was not a result of (i) reduced surface expression, (ii) reduced agonist potency or (iii), elevated basal signaling activity. Evidence of a possible ionic interaction between Asp^{148}-Arg^{149} appears unlikely as the double mutant (D148R/R149D), which reversed these two charges, failed to be expressed on the surface and was unable to bind ligands or signal.

Charged residues located near the boundaries of TM regions are often important for the topology of membrane-spanning proteins (Rutz et al., 1999). For GPCRs, Asp(3.49) and Arg(3.50) residues are located at the interface of TM-III-IC2. It is probable that mutations of either residue disturbs the charge balance at this position and destabilize the α-helical structure of TM-III and/or with phospholipids. This could exert deleterious effects on cell surface expression and impair interactions with G-protein(s), access for phosphorylation by kinases and/or recruitment of regulatory proteins mediating internalization. In this regard, Glu/Asp residues are always conserved and where studied, glutamyl is often an effective substitution for Asp(3.49) (Auger et al., 2002). This is consistent with the V_{1a}R, where Glu^{148} was able to bind ligands and signal, but not with other substitutions. Conservative replacements of Arg(3.50)

Molecular Pharmacology Fast Forward. Published on July 27, 2005 as DOI: 10.1124/mol.105.013359
This article has not been copyedited and formatted. The final version may differ from this version.

are well tolerated amongst some GPCRs (e.g. Lys^{129} in thromboxane A_2 receptors (Capra et al., 2004)). In contrast, opposing charges can be detrimental, demonstrated by the lack of surface expression when an aspartyl residue was present. Furthermore, the position of these residues within the motif was crucial as [D148R/R149D]V_{1a}R failed to reach the surface. Conversely, the conservative histidyl substitution was an effective replacement for Arg^{149} albeit with a slightly reduced expression and signaling ability. A mutation identified in V_2Rs (R137H) of some patients with NDI was reported to be constitutively internalized and co-localized with β-arrestin (Barak et al., 2001). Interestingly, the corresponding mutant reported here ([R149H]V_{1a}R) showed a significantly increased rate and amount of receptor internalized without any elevated signaling activity. One possibility is that this mutant may display an enhanced affinity for β-arrestin and/or for other regulatory proteins involved in this process. Interestingly, a mutant (R123G) in the DRY motif of the N-formyl peptide receptor disrupted normal β-arrestin binding whilst still being able to internalize (Bennett et al., 2000). Consequently, the role of the Arg(3.50) in the V_{1a}R (and other GPCRs) may extend to regulating other important aspects of receptor function.

Mutation of tyrosyl (3.51) had little effect on binding ligands, signaling and receptor internalization. A reduced maximal signaling ability was observed which was similar to other Arg^{149} substitutions. The functional role of Tyr(3.51) has been studied in detail for m1 mAChRs, which reported reduced expression and a strong preference for aromatic residues (Lu et al., 1997). In general, Tyr(3.51) has not been extensively studied with only minor effects on receptor function being reported.

In summary, this study has demonstrated the importance of specific residues within the highly conserved DRY motif in the $V_{1a}R$ for ligand-binding, signaling, cell surface delivery and agonist-mediated internalization. An aspartyl (3.49) was critical for surface delivery and function. A glutamyl partially restored expression, but receptor stability at the surface was reduced with a greater tendency of receptors to be internalized. In contrast to most GPCRs, Arg(3.50) (and Tyr(3.51)) were not essential for expression, agonist-binding or coupling to $G\alpha_{q/11}$, although maximal signaling responses were impaired. A histidyl at position (3.50) did reveal a role for agonist-mediated internalization of $V_{1a}Rs$. Although the DRY motif amongst GPCRs is highly conserved, its role in the general mechanism of GPCR activation and signaling are likely to be receptor and subtype specific.

Molecular Pharmacology Fast Forward. Published on July 27, 2005 as DOI: 10.1124/mol.105.013359
This article has not been copyedited and formatted. The final version may differ from this version.

Acknowlegments

I am grateful to Dr. Claudine Serradeil-Le Gal (Sanofi Recherche, France) for providing a sample of SR 49059 and to Prof. S. J. Hill (Institute of Cell Signalling, University of Nottingham) for critical reading and comments on the manuscript. I am grateful to Tim Self (Institute of Cell Signalling, University of Nottingham) for excellent technical assistance with the confocal microscopy.

Molecular Pharmacology Fast Forward. Published on July 27, 2005 as DOI: 10.1124/mol.105.013359
This article has not been copyedited and formatted. The final version may differ from this version.

References

Alewijnse AE, Timmerman H, Jacobs EH, Smit MJ, Roovers E, Cotecchia S, and Leurs R (2000) The effect of mutations in the DRY motif on the constitutive activity and structural instability of the histamine H(2) receptor. *Mol Pharmacol* **57:** 890-898.

Arora KK, Cheng Z, and Catt KJ (1997) Mutations of the conserved DRS motif in the second intracellular loop of the gonadotropin-releasing hormone receptor affect expression, activation, and internalization. *Mol Endocrinol* **11:**1203-1212.

Auger GA, Pease JE, Shen X, Xanthou G, Barker MD (2002) Alanine scanning mutagenesis of CCR3 reveals that the three intracellular loops are essential for functional receptor expression. *Eur J Immunol*. 32:1052-1058.

Ballesteros JA, and Weinstein H (1995) Integrated methods for the construction of three-dimensional models and computational probing of structure-function relations in G protein-coupled receptors *Methods Neurosci* **25:**366-428.

Ballesteros J, Kitanovic S, Guarnieri F, Davies P, Fromme BJ, Konvicka K, Chi L, Millar RP, Davidson JS, Weinstein H, and Sealfon SC (1998) Functional microdomains in G-protein-coupled receptors. The conserved arginine-cage motif in the gonadotropin-releasing hormone receptor. *J Biol Chem* **273:**10445-10453.

Barak LS, Oakley RH, Laporte SA, and Caron MG (2001) Constitutive arrestin-mediated desensitization of a human vasopressin receptor mutant associated with nephrogenic diabetes insipidus. *Proc Natl Acad Sci* **98:**93-98.

Bowen-Pidgeon D, Innamorati G, Sadeghi HM, and Birnbaumer M (2001) Arrestin effects on internalization of vasopressin receptors. *Mol Pharmacol* **59:**1395-1401.

Capra V, Veltri A, Foglia C, Crimaldi L, Habib A, Parenti M, and Rovati GE (2004) Mutational analysis of the highly conserved ERY motif of the thromboxane A2 receptor: alternative role in G protein-coupled receptor signaling. *Mol Pharmacol* **66:**880-889.

Cheng Y, and Prusoff WH (1973) Relationship between the inhibition constant (K1) and the concentration of inhibitor which causes 50 per cent inhibition (I50) of an enzymatic reaction. *Biochem Pharmacol* **22:**3099-3108.

Chung DA, Wade SM, Fowler CB, Woods DD, Abada PB, Mosberg HI, and Neubig RR (2002) Mutagenesis and peptide analysis of the DRY motif in the alpha2A adrenergic receptor: evidence for alternate mechanisms in G protein-coupled receptors. *Biochem Biophys Res Commun* **293:**1233-1241.

Costa EM, Bedecarrats GY, Mendonca BB, Arnhold IJ, Kaiser UB, and Latronico AC (2001) Two novel mutations in the gonadotropin-releasing hormone receptor gene in Brazilian

patients with hypogonadotropic hypogonadism and normal olfaction. *J Clin Endocrinol Metab* **86:**2680-2686.

Fanelli F, Barbier P, Zanchetta D, de Benedetti PG, and Chini B (1999) Activation mechanism of human oxytocin receptor: a combined study of experimental and computer-simulated mutagenesis. *Mol Pharmacol* **56:**214-225.

Hawtin SR, and Wheatley M (1997) Characterization of an epitope-tagged vasopressin receptor: A probe for receptor structure and function. *Biochem Soc Trans* **25:**437S.

Hawtin SR, Tobin A, Patel S, and Wheatley M (2001) A Palmitoylation-defective Mutation of the Vasopressin V_{1a} Receptor Reveals a Functional Role for Acylation in Receptor Phosphorylation and Internalization. *J Biol Chem* **276:**38139-38146.

Hawtin SR, Wesley VJ, Parslow RA, Simms J, Miles A, McEwan K, and Wheatley M (2002) A Single Residue (Arg^{46}) Located Within the N-terminus of the V_{1a} vasopressin receptor Is Critical for Binding Vasopressin But Not Peptide or Nonpeptide Antagonists. *Mol Endocrinol* **16:**600-609.

Gimpl G, and Fahrenholz F (2001) The oxytocin receptor system: structure, function, and regulation. *Physiol Rev* **81:**629-683.

Jones PG, Curtis CA, and Hulme EC (1995) The function of a highly-conserved arginine residue in activation of the muscarinic M1 receptor. *Eur J Pharmacol* **288:**251-257.

Karnik SS, Gogonea C, Patil S, Saad Y, and Takezako T (2003) Activation of G-protein-coupled receptors: a common molecular mechanism. *Trends Endocrinol Metab* **14:**431-437.

Kristiansen K (2003) Molecular mechanisms of ligand binding, signaling, and regulation within the superfamily of G-protein-coupled receptors: molecular modeling and mutagenesis approaches to receptor structure and function. *Pharmacol Ther* **103:**21-80.

Kruszynski M, Lammek B, Manning M, Seto J, Haldar J, and Sawyer WH (1980) [1-beta-Mercapto-beta,beta-cyclopentamethylenepropionic acid),2-(O-methyl)tyrosine]argine-vasopressin and [1-beta-mercapto-beta,beta-cyclopentamethylenepropionic acid)]argine-vasopressine, two highly potent antagonists of the vasopressor response to arginine-vasopressin. *J Med Chem* **23:**364-368.

Lu ZL, Curtis CA, Jones PG, Pavia J, and Hulme EC (1997) The role of the aspartate-arginine-tyrosine triad in the m1 muscarinic receptor: mutations of aspartate 122 and tyrosine 124 decrease receptor expression but do not abolish signaling *Mol Pharmacol* **51:** 234-241.

Liu J, and Wess J (1996) Different single receptor domains determine the distinct G protein coupling profiles of members of the vasopressin receptor family. *J Biol Chem* **271:**8772-8778.

Milligan G (2003) Constitutive activity and inverse agonists of G protein-coupled receptors: a current perspective. *Mol Pharmacol* **64:**1271-1276.

Morello JP, and Bichet DG (2001) Nephrogenic diabetes insipidus. *Annu Rev Physiol* **63:**607-630.

Morin D, Cotte N, Balestre MN, Mouillac B, Manning M, Breton C, and Barberis C (1998) The D136A mutation of the V2 vasopressin receptor induces a constitutive activity which permits discrimination between antagonists with partial agonist and inverse agonist activities. *FEBS Lett* **441:**470-475.

Palczewski K, Kumasaka T, Hori T, Behnke CA, Motoshima H, Fox BA, Le Trong I, Teller DC, Okada T, Stenkamp RE, Yamamoto M, and Miyano M (2000) Crystal structure of rhodopsin: A G protein-coupled receptor. *Science* **289:**739-745.

Parnot C, Miserey-Lenkei S, Bardin S, Corvol P, and Clauser E (2002) Lessons from constitutively active mutants of G protein-coupled receptors. *Trends Endocrinol Metab* **13:**336-343.

Rasmussen SG, Jensen AD, Liapakis G, Ghanouni P, Javitch JA, and Gether U (1999) Mutation of a highly conserved aspartic acid in the beta2 adrenergic receptor: constitutive activation, structural instability, and conformational rearrangement of transmembrane segment 6. *Mol Pharmacol* **56:**175-184.

Rutz C, Rosenthal W, and Schulein R (1999) A single negatively charged residue affects the orientation of a membrane protein in the inner membrane of Escherichia coli only when it is located adjacent to a transmembrane domain. *J Biol Chem* **274:**33757-33763.

Scheer A, Costa T, Fanelli F, De Benedetti PG, Mhaouty-Kodja S, Abuin L, Nenniger-Tosato M, and Cotecchia S (2000) Mutational analysis of the highly conserved arginine within the Glu/Asp-Arg-Tyr motif of the alpha(1b)-adrenergic receptor: effects on receptor isomerization and activation. *Mol Pharmacol* **57:**219-231.

Scheer A, Fanelli F, Costa T, De Benedetti PG, and Cotecchia S (1996) Constitutively active mutants of the alpha 1B-adrenergic receptor: role of highly conserved polar amino acids in receptor activation. *EMBO J* **15:**3566-3578.

Scheer A, Fanelli F, Costa T, De Benedetti PG, and Cotecchia S (1997) The activation process of the alpha1B-adrenergic receptor: potential role of protonation and hydrophobicity of a highly conserved aspartate. *Proc Natl Acad Sci* USA **94:**808-813.

Schmidt A, Audigier S, Barberis C, Jard S, Manning M, Kolodziejczyk AS, and Sawyer WH (1991) A radioiodinated linear vasopressin antagonist: a ligand with high affinity and specificity for V1a receptors. *FEBS Lett* **282:**77-81.

Serradeil-Le Gal C, Wagnon J, Garcia C, Lacour C, Guiraudou P, Christophe B, Villanova G, Nisato D, Maffrand JP, and Le Fur G (1993) Biochemical and pharmacological properties of SR 49059, a new, potent, nonpeptide antagonist of rat and human vasopressin V1a receptors. *J Clin Invest* **92:**224-231.

Smit MJ, Leurs R, Alewijnse AE, Blauw J, Van Nieuw Amerongen GP, Van De Vrede Y, Roovers E, and Timmerman H (1996) Inverse agonism of histamine H2 antagonist accounts for upregulation of spontaneously active histamine H2 receptors. *Proc Natl Acad Sci* USA. **93:**6802-6807.

Tan CM, Brady AE, Nickols HH, Wang Q, and Limbird LE (2004) Membrane trafficking of G protein-coupled receptors. *Annu Rev Pharmacol Toxicol* **44:**559-609.

Thibonnier M, Coles P, Thibonnier A, and Shoham M (2001a) The basic and clinical pharmacology of nonpeptide vasopressin receptor antagonists. *Annu Rev Pharmacol Toxicol* **41:**175-202.

Thibonnier M, Plesnicher CL, Berrada K, and Berti-Mattera L (2001b) Role of the human V1 vasopressin receptor COOH terminus in internalization and mitogenic signal transduction. *Am J Physiol Endocrinol Metab* **281:**E81-92.

Wilbanks AM, Laporte SA, Bohn LM, Barak LS, and Caron MG (2002) Apparent loss-of-function mutant GPCRs revealed as constitutively desensitized receptors. *Biochemistry* **41:**11981-11989.

Wong SK (2003) G protein selectivity is regulated by multiple intracellular regions of GPCRs. *Neurosignals* **12:**1-12.

Molecular Pharmacology Fast Forward. Published on July 27, 2005 as DOI: 10.1124/mol.105.013359
This article has not been copyedited and formatted. The final version may differ from this version.

Footnotes

This work was supported by an independent fellowship awarded from the University of Nottingham

Molecular Pharmacology Fast Forward. Published on July 27, 2005 as DOI: 10.1124/mol.105.013359
This article has not been copyedited and formatted. The final version may differ from this version.

Legends for figures

Fig. 1. Schematic Diagram of the $V_{1a}R$. TMs are shown as cylinders transversing the lipid bilayer. The position of the engineered HA-epitope tag is indicated. Branched structures indicate the positions of N-glycosylation sites. The couplet comprising Cys^{371}/Cys^{372} is palmitoylated (Hawtin et al., 2001) and is shown forming an additional membrane anchor point which results in a fourth intracellular loop containing an α-helical segment parallel to the membrane. The sequence and position in the receptor of the "DRY" motif and IC2 is indicated by the enlarged insert. Sequence alignment (obtained from SwisProt PDB and GenEMBL) of the distal region of TM-III, the conserved "DRY" motif (bold) and IC2 for human $V_{1a}R$, OTR, $V_{1b}R$ and V_2Rs are shown.

Fig. 2. Comparison of Functional Coupling of Alanyl Substituted "DRY" Mutant Receptors. Panel (**A**), AVP-induced accumulation of mono-, bis-, and trisphosphates in HEK 293T cells transiently transfected with wild-type $V_{1a}R$, (●); [R149A]$V_{1a}R$, (■); or [Y150A]$V_{1a}R$, (▼). Values are stimulation induced by AVP at the stated concentrations expressed as percent maximum. Panel (**B**), EC_{50} and E_{max} (fold maximum stimulation over basal) values of Wt and mutant receptors. Data shown is mean ± S.E.M. of three individual experiments (unless otherwise stated (*n*)) each performed in triplicate. [a]Not a true E_{max}, fold-stimulation of [D148A]$V_{1a}R$ was determined with 10 μM AVP. ND=None detected. ** $p<0.01$ compared to wild-type $V_{1a}R$ using ANOVA with a post hoc Dunnett's test analysis (GraphPad Prism4).

Molecular Pharmacology Fast Forward. Published on July 27, 2005 as DOI: 10.1124/mol.105.013359
This article has not been copyedited and formatted. The final version may differ from this version.

Fig. 3. Cell Surface Localization of Wild-type and Ala^{148} Receptors. HEK 293T cells were transiently transfected with either pcDNA3 vector alone (**A, B**), HA-tagged Wt $V_{1a}R$ (**C, D**) or [D148A]$V_{1a}R$ (**E, F**). Cells were fixed in 3 % (v/v) paraformaldehyde and processed for immmunocytochemistry as described in "Materials and Methods". Phase images (**A, C** and **E**) or excitation (543 nm) with the HeNe laser and a 560 nm long pass emission filter (**B, D and F**) are shown. Images shown are representative from three separate experiments.

Fig. 4. Internalization of Wild-type and Alanyl Substituted "DRY" Mutant Receptors. Panel **(A),** AVP-induced internalization of HEK 293T cells transiently transfected with wild-type $V_{1a}R$, (●); [R149A]$V_{1a}R$, (■); or [Y150A]$V_{1a}R$, (▼). Cells were stimulated with 1 μM AVP at 37 °C to promote internalization and incubated (with AVP) for appropriate time intervals indicated (over a maximum 60 min period). Total number of receptors remaining at the cell surface was measured by ELISA as described in 'Materials and Methods'. Panel (**B**), maximum (%) of each receptor internalized following AVP treatment (1 μM) for 60 min is shown. The time ($t_{1/2}$ min) for 50 % of each receptor that can be internalized is indicated. Data shown are the mean ± S.E.M. of three separate experiments (unless otherwise stated (*n*)) each performed in triplicate.

Fig. 5. Cell Surface Expression of Asp^{148} and Arg^{149} Substituted Mutant Receptors. HEK 293T cells were transiently transfected with Panel (**A**), wild-type $V_{1a}R$, [D148A]$V_{1a}R$, [D148N]$V_{1a}R$ and [D148E]$V_{1a}R$; or Panel (**B**), wild-type $V_{1a}R$,

Molecular Pharmacology Fast Forward. Published on July 27, 2005 as DOI: 10.1124/mol.105.013359
This article has not been copyedited and formatted. The final version may differ from this version.

[R149A]V_{1a}R, [R149D]V_{1a}R and [R149H]V_{1a}R. Total number of receptors remaining at the cell surface was quantified by ELISA as described in 'Materials and Methods'. Data shown is mean ± S.E.M. of (*n*) individual experiments each performed in triplicate. ** $p<0.01$ compared to Wt V_{1a}R using ANOVA with a post hoc Dunnett's test analysis (GraphPad Prism4).

Fig. 6. Comparison of Functional Coupling of Asp[148] and Arg[149] Substituted Mutant Receptors. AVP-induced accumulation of mono-, bis-, and trisphosphates in HEK 293T cells transiently transfected with Panel (**A**), wild-type V_{1a}R, (●) and [D148E]V_{1a}R, (△); or Panel (**B**), wild-type V_{1a}R, (●) and [R149H]V_{1a}R, (□). Values are stimulation induced by AVP at the stated concentrations expressed as percent maximum. Panel (**C**), EC_{50} and E_{max} (fold maximum stimulation over basal) values of Wt and mutant receptors. Data shown is mean ± S.E.M. of three individual experiments (unless otherwise stated (*n*)) each performed in triplicate. ND=None detected. ** $p<0.01$ compared to Wt V_{1a}R using ANOVA with a post hoc Dunnett's test analysis (GraphPad Prism4). [a]Not a true E_{max}, fold-stimulation of [D148N]V_{1a}R, [D148R]V_{1a}R, [R149D]V_{1a}R and [D148R/R149D]V_{1a}R was determined with 10 μM AVP.

Fig. 7. Internalization of Wild-type and Glu[148] and His[149] Substituted Mutant Receptors. AVP-induced internalization of HEK 293T cells transiently transfected with Panel (**A**), wild-type V_{1a}R, (●) and [D148E]V_{1a}R, (△); or Panel (**B**), wild-type V_{1a}R, (●) and [R149H]V_{1a}R, (□). Cells were stimulated with 1 μM AVP at 37 °C to promote internalization and incubated (with AVP) for appropriate time intervals indicated (over a

maximum 60 min period). Total number of receptors remaining at the cell surface was measured by ELISA as described in 'Materials and Methods'. Panel (**C**), maximum (%) of each receptor internalized following continuous AVP stimulation (1 μM) at 37 °C for 60 min. The time ($t_{1/2}$ min) for 50 % of each receptor that can be internalized is indicated. Data shown are the mean ± S.E.M. of three separate experiments (unless otherwise stated (*n*)) each performed in triplicate. **p*<0.05 and ** *p*<0.01 compared to Wt $V_{1a}R$ using ANOVA with a post hoc Dunnett's test analysis (GraphPad Prism4).

Molecular Pharmacology Fast Forward. Published on July 27, 2005 as DOI: 10.1124/mol.105.013359
This article has not been copyedited and formatted. The final version may differ from this version.

TABLE 1. Pharmacological Profile of Alanyl-substituted "DRY" Mutant V_{1a}Rs.

Mutant V_{1a}Rs were expressed in HEK 293T cells and characterized pharmacologically. Dissociation constants (K_i) were calculated from IC_{50} values and corrected for radioligand occupancy as described in "Materials and Methods". CA=cyclic peptide antagonist, LA=linear peptide antagonist, SR49059 = non-peptide antagonist. ND=none detected. Cell surface expression of each mutant was quantified in parallel by ELISA and expressed as % HA-tagged Wt V_{1a}R. Data shown is mean ± S.E.M. of three individual experiments (unless otherwise stated (*n*)) with each performed in triplicate. Cell surface expression of 100 % corresponds to ~0.8 pmoles/mg membrane protein.

	Binding affinities K_i (nM)				
Receptor	AVP (agonist)	CA (Antagonist)	LA (Antagonist)	SR 49059 (Antagonist)	Cell surface expression (% Wt)
Wt	1.0 ± 0.1	0.5 ± 0.1	0.2 ± 0.01	0.7 ± 0.1	100
D148A	ND	ND	ND	ND	2 ± 2 (7)
R149A	2.6 ± 0.4	1.4 ± 0.3	1.2 ± 0.1	1.9 ± 0.2	101 ± 5 (5)
Y150A	1.3 ± 0.3	1.0 ± 0.2	0.4 ± 0.1	1.3 ± 0.2	91 ± 4 (6)

Molecular Pharmacology Fast Forward. Published on July 27, 2005 as DOI: 10.1124/mol.105.013359
This article has not been copyedited and formatted. The final version may differ from this version.

TABLE 2. Pharmacological Profile of Substituted Asp[148] and Arg[149] Mutant V_{1a}Rs.

Mutant V_{1a}Rs were expressed in HEK 293T cells and characterized pharmacologically. Dissociation constants (K_i) were calculated from IC_{50} values and corrected for radioligand occupancy as described in "Materials and Methods". CA=cyclic peptide antagonist, LA=linear peptide antagonist, SR49059=non-peptide antagonist. ND=none detected. Cell surface expression of each mutant was quantified in parallel by ELISA and expressed as % HA-tagged Wt V_{1a}R. Data shown is mean ± S.E.M. of three individual experiments (unless otherwise stated (*n*)) with each performed in triplicate. Cell surface expression of 100 % corresponds to ~0.8 pmoles/mg membrane protein.

	Binding affinities K_i (nM)				
Receptor	AVP (agonist)	CA (Antagonist)	LA (Antagonist)	SR 49059 (Antagonist)	Cell surface expression (% Wt)
Wt	1.0 ± 0.1	0.5 ± 0.1	0.2 ± 0.0	0.7 ± 0.1	100
D148N	ND	ND	ND	ND	19 ± 2 (5)
D148E	4.5 ± 1.1 (4)	1.4 ± 0.3	0.3 ± 0.1	1.7 ± 0.5	43 ± 4 (9)
D148R	ND	ND	ND	ND	3 ± 0 (4)
R149D	ND	ND	ND	ND	5 ± 4 (6)
R149H	3.5 ± 0.3	1.0 ± 0.2	0.4 ± 0.0	2.0 ± 0.2	63 ± 5 (8)
D148R/R149D	ND	ND	ND	ND	2 ± 1 (4)

Molecular Pharmacology Fast Forward. Published on July 27, 2005 as DOI: 10.1124/mol.105.013359
This article has not been copyedited and formatted. The final version may differ from this version.

Fig. 1

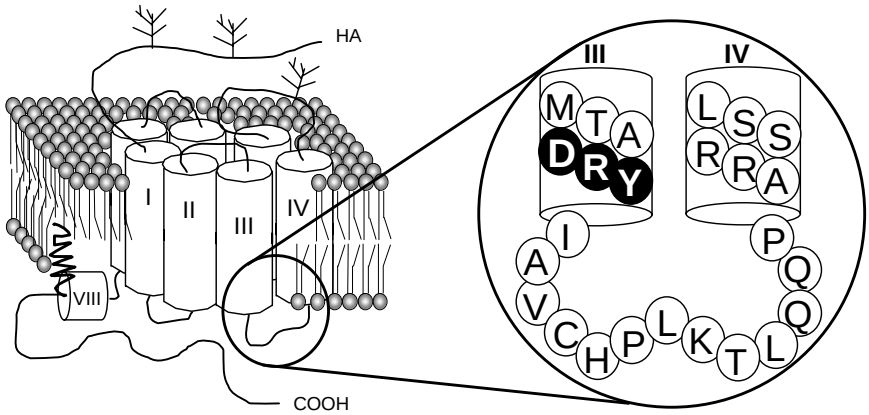

	TM-III IC2
$V_{1a}R$:	MTA**DRY**-IAVCHPLKTLQQP
OTR:	MSL**DRC**-LAICQPLRSLRRR
V_2R:	MTA**DRH**-RAICRPMLAYRHG
$V_{1b}R$:	MTL**DRY**-LAVCHPLRSLQQP

Molecular Pharmacology Fast Forward. Published on July 27, 2005 as DOI: 10.1124/mol.105.013359
This article has not been copyedited and formatted. The final version may differ from this version.

Fig. 2

(A)

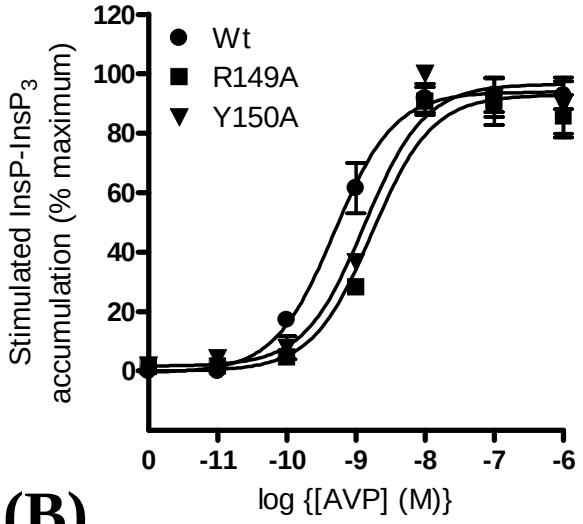

(B)

	Stimulation of InsP – $InsP_3$	
Receptor	EC_{50} (nM)	E_{max} (fold)
Wt	0.6 ± 0.2	5.8 ± 0.9 (8)
D148A	ND	1.6 ± 0.2 (5)[a]**
R149A	1.8 ± 0.2	2.5 ± 0.4**
Y150A	1.2 ± 0.2	2.9 ± 0.4**

Molecular Pharmacology Fast Forward. Published on July 27, 2005 as DOI: 10.1124/mol.105.013359
This article has not been copyedited and formatted. The final version may differ from this version.

Fig. 3

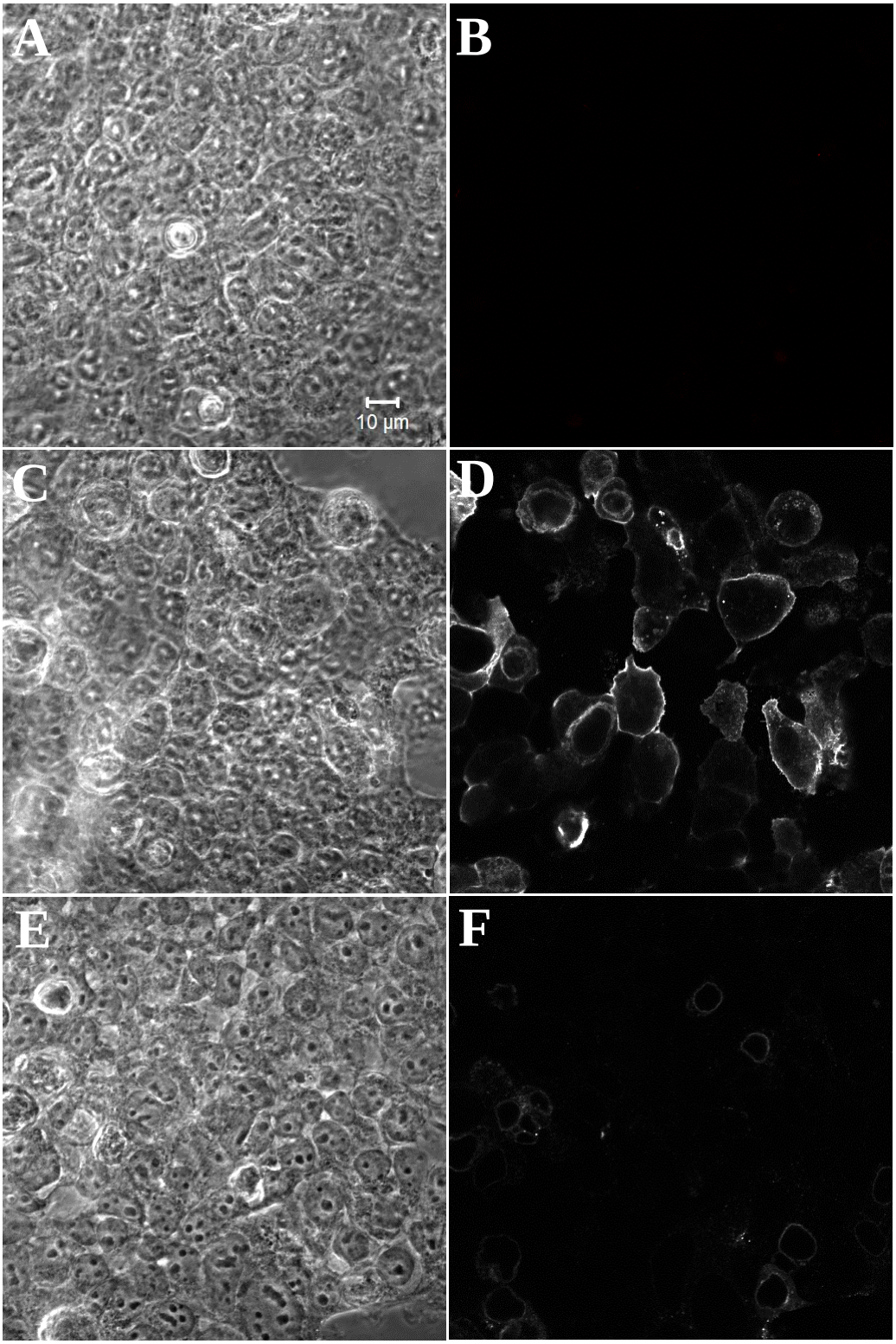

Molecular Pharmacology Fast Forward. Published on July 27, 2005 as DOI: 10.1124/mol.105.013359
This article has not been copyedited and formatted. The final version may differ from this version.

Fig. 4

(A)

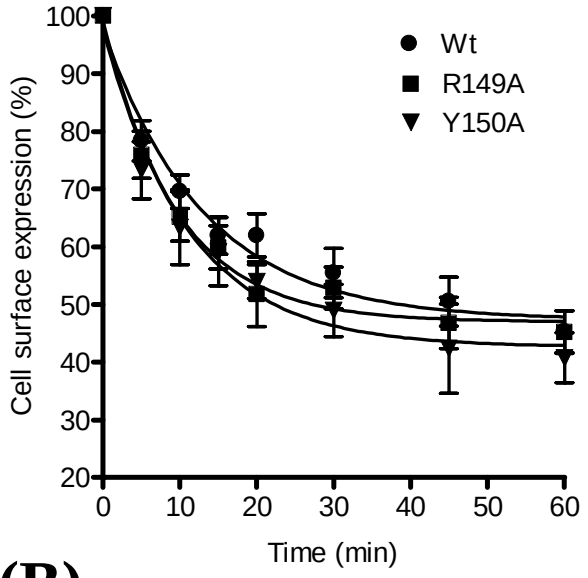

(B)

	AVP-mediated internalization	
Receptor	% Maximum	Rate ($t_{1/2}$) min
Wt	59 ± 2 (8)	9.9 ± 1.0 (6)
R149A	58 ± 3 (7)	6.8 ± 1.0
Y150A	61 ± 2 (6)	7.9 ± 1.4

Molecular Pharmacology Fast Forward. Published on July 27, 2005 as DOI: 10.1124/mol.105.013359
This article has not been copyedited and formatted. The final version may differ from this version.

Fig. 5

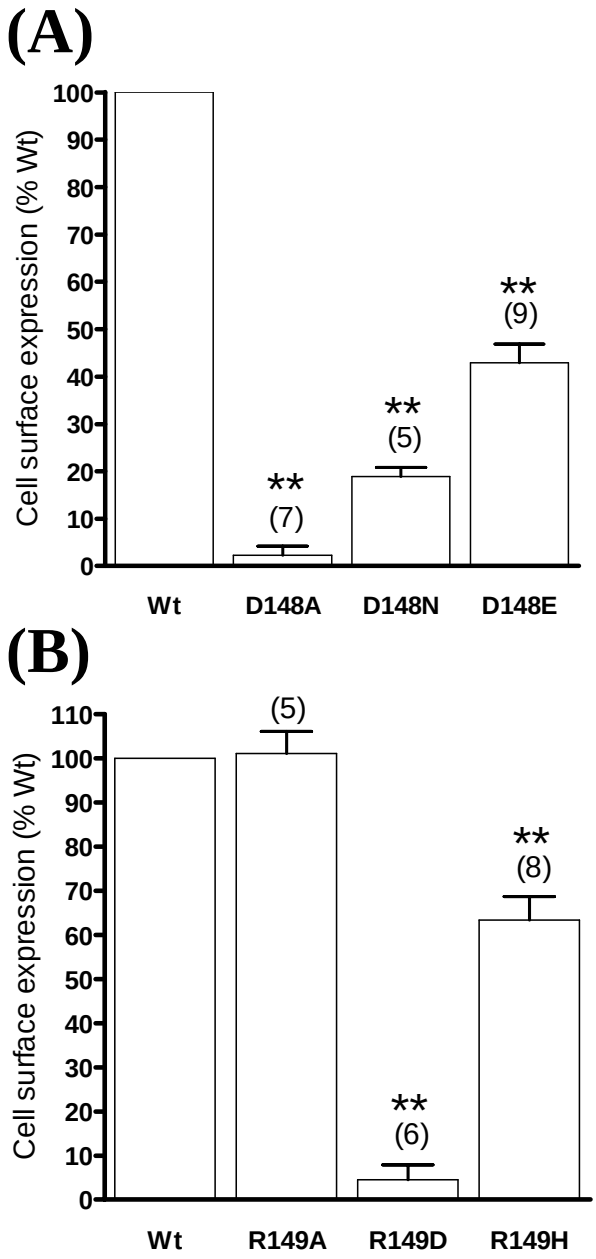

Molecular Pharmacology Fast Forward. Published on July 27, 2005 as DOI: 10.1124/mol.105.013359
This article has not been copyedited and formatted. The final version may differ from this version.

Fig. 6

(A)

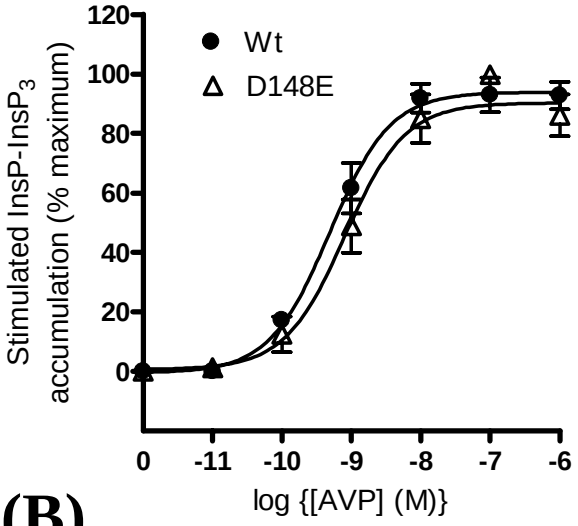

(B)

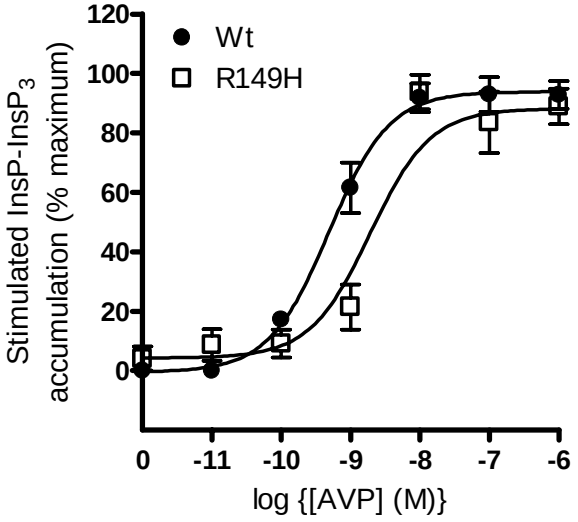

(C)

	Stimulation of InsP – $InsP_3$	
Receptor	EC_{50} (nM)	E_{max} (fold)
Wt	0.6 ± 0.2	5.8 ± 0.9 (8)
D148N	ND	1.7 ± 0.2 (5)[a]**
D148E	0.9 ± 0.2	2.5 ± 0.3 (6)**
D148R	ND	1.2 ± 0.1 (3)[a]**
R149D	ND	1.1 ± 0.1(6)[a]**
R149H	2.2 ± 0.7	1.8 ± 0.1 (5)**
D148R/R149D	ND	1.0 ± 0.1 (3)[a]**

Molecular Pharmacology Fast Forward. Published on July 27, 2005 as DOI: 10.1124/mol.105.013359
This article has not been copyedited and formatted. The final version may differ from this version.

Fig. 7

(A)

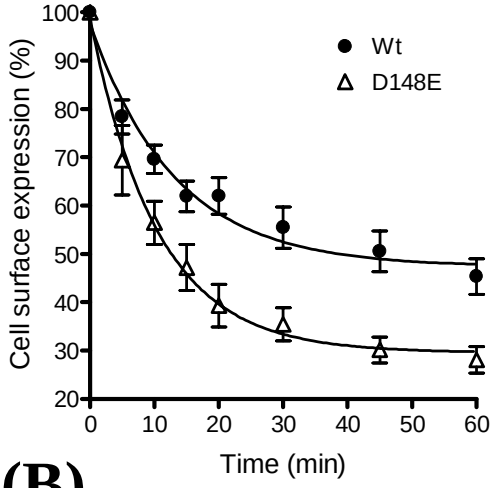

(B)

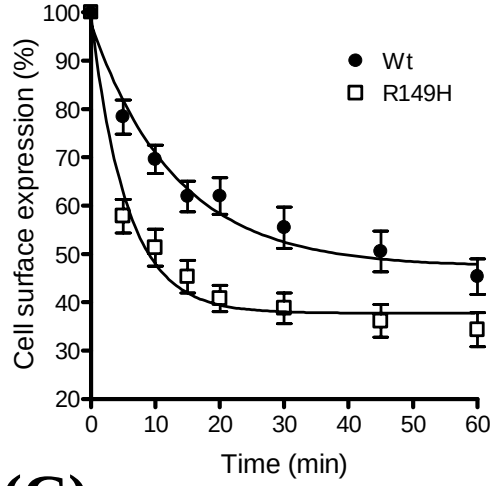

(C)

	AVP-mediated internalization	
Receptor	% Maximum	Rate ($t_{1/2}$) min
Wt	59 ± 2 (8)	9.9 ± 1.0 (6)
D148E	77 ± 2**	7.4 ± 1.1
R149H	70 ± 2 (6)*	4.0 ± 0.5 (5)**